Analyzing Potential Risk of Wind-Induced Damage in Construction Sites and Neighboring Communities Using Large-Scale Visual Data from Drones

Mirsalar Kamari[1] and Youngjib Ham[2]

[1]Ph.D. Student, Dept. of Construction Science, Texas A&M Univ., College Station, TX. E-mail: kamari@tamu.edu
[2]Assistant Professor, Dept. of Construction Science, Texas A&M Univ., College Station, TX. E-mail: yham@tamu.edu

ABSTRACT

Dynamic and complex construction sites including incomplete structures and unsecured resources are among the most vulnerable environments to windstorms such as hurricanes. To better secure unstructured construction sites, this paper aims at proposing a new vision-based method to analyze potential risk of wind-induced damage in construction sites. First, by leveraging large-scale images collected from drones, we reconstruct a 3D point cloud model of construction sites and perform the semantic segmentation to categorize potential wind-borne debris. Then, we identify the positions of the potential wind-borne debris given wind speeds and perform the volumetric measurement on such vulnerable objects. Finally, building on the position and the volume of the potential wind-borne debris, we quantify the associated threat level in the context of their kinetic energy in wind situations. A case study was conducted on a real construction site to validate the proposed method. The proposed imaging-to-simulation framework enables practitioners to automatically flag vulnerable objects/areas in construction sites with respect to the severity of wind events, which helps better secure their jobsites in a timely manner before potential extreme wind events in order to minimize the associated damage.

INTRODUCTION

In the United States, extreme wind events such as hurricanes and tropical storms are among the costliest natural disasters (Smith and Katz 2013). According to National Oceanic and Atmospheric Administration (NOAA), in the year of 2017, more than 306 billion dollars in damage were induced by 16 strong wind/weather-related events throughout the United States. Being responsible for 161 billion dollars of damage, hurricane Harvey was the most devastating after hurricane Maria and Irma with total of 90 and 50 billion dollars of damage in 2017 (National-Oceanic-and-Atmospheric-Administration 2018). Beside the massive economical damage, more importantly, a total of 2075 life loss caused by hurricane Maria represents a large human toll (Willison et al. 2019).

Historically, such significant threat has had catastrophic impact on the construction industry. Structured elements are usually not the main victims in the extreme wind events such as hurricanes, because they typically satisfy sets of standards, namely the building codes, and thus, no structural damages and failures are typically expected to take place. Rather, the majority of wind-induced damages are occurred due to the collision impact of flying debris (Lee 1988; Minor 1994). Wind-borne debris have induced a devastated level of damage to communities. In the year of 1983, due to the aftermath of Hurricane Alicia, approximately 3000 façade panels of the Wells Fargo Plaza building (also known as the Allied Bank Plaza, located in Houston, TX) had been replaced. Later, the inspections indicated that the glass panel failures were primarily induced by the collision impact of flying debris (Kareem 1986). In this regard, it is no wonder

that construction sites, consisting of incomplete structures and unsecured resources, are recognized as one of the most susceptible environments to severe wind-related events (Ham et al. 2017). For instance, in the year of 2012, the aftermath of hurricane Sandy left ~185 million dollars in damage to the World Trade Center construction project (Fermino 2013). Generally, any loose material or resources in construction sites can become potential wind-borne debris, which may cause economic damage and a loss of life if they are lifted off the ground by strong winds. Considering such huge impact that could pose a serious threat, municipal agencies require practitioners to take proper actions to secure their construction sites before extreme wind events to minimize the associated damage. Thus, it is significant to quickly detect potential wind-borne debris in construction sites and robustly take proactive safety measures.

Meanwhile, the advent of digital cameras and camera-equipped platforms such Unmanned Aerial Vehicles (UAVs) has encouraged the construction industry to collect and use large-scale photos or videos to conduct meaningful visual analytics to check safety requirements and perform quality control (Asadi et al. 2019; Asadi et al. 2018; Ham and Kamari 2019; Kamari and Ham 2018). In this paper, by leveraging images collected from UAVs, we identify and analyze potential wind-born debris in construction sites with respect to different wind speeds, aiming to better secure the jobsites and promote the safety of the construction project. The proposed method has the following workflow: 1) perform 3D dense reconstruction of construction sites and detect potential wind-borne debris on the sites in order to characterize the states of the at-risk construction sites; 2) carry out the volumetric measurement of vulnerable objects as potential wind-borne debris pose a great threat to construction projects as well as neighboring communities in extreme wind events; and 3) calculate the kinetic energy associated with potential wind-borne debris to quantify the potential threat once they become airborne, by taking into account the volume and density of the detected potential debris. A heatmap is generated to visualize the vulnerability associated with potential wind-borne debris in construction sites in different wind speeds. The outcomes of the proposed method will give practitioners a heads up of the most likely scenarios that need to be analyzed for decision-making in extreme wind events, which enables to better secure their construction sites in a limited time frame and resource for preparedness.

BACKGROUND

Prior works on disaster management efforts can be divided into pre- and post-management. The main focus of the post-disaster management is rapid damage assessments such as (Hatzikyriakou et al. 2015) or recovery planning such as (Esmalian et al. 2019). Contrarily, the pre-disaster management are geared toward adapting mitigation and preparedness plans through proactive risk assessments. In the context of wind-borne debris and related potential risk, for example, (Minor 1994) evaluated the risk of wind-borne debris in the severe wind events to the neighboring community. Later, (Wills et al. 2002) were the first to categorize the shape of wind-borne debris (e.g., sphere, sheet and rod types) and mathematically reasons the dynamics of the associated problems. Building upon the prior works, the characteristics of sheet and rod type debris have been further studied by (Holmes 2004; Holmes et al. 2006) to incorporate the rotational moments in the trajectories of such debris. Despite the benefits of such theoretical approaches, in practice, labor-intensive human effort is required to characterize the states of at-risk environments involving potential wind-borne debris for proactive analysis. In other words, to carry out risk assessments, human supervision is needed to determine what potential debris are located where and what particular characteristics they inherit. To address this knowledge gap,

there is a need for identifying the position of potential wind-borne debris in construction sites and quantifying their threat level robustly.

PROPOSED METHOD

By leveraging large-scale images collected from UAVs, the objective of this paper is to automatically identify and analyze potential wind-induced damage in construction sites, prior to extreme wind events. Figure 1 illustrates the proposed method which consists of three main modules: 1) 3D reconstruction and semantic segmentation of potential wind-borne debris as Regions of Interests (ROIs); 2) volumetric measurement over the ROIs; and 3) calculation of the kinetic energy for each ROI given a specific wind speed. All of the aforementioned modules are elaborated in the following sections.

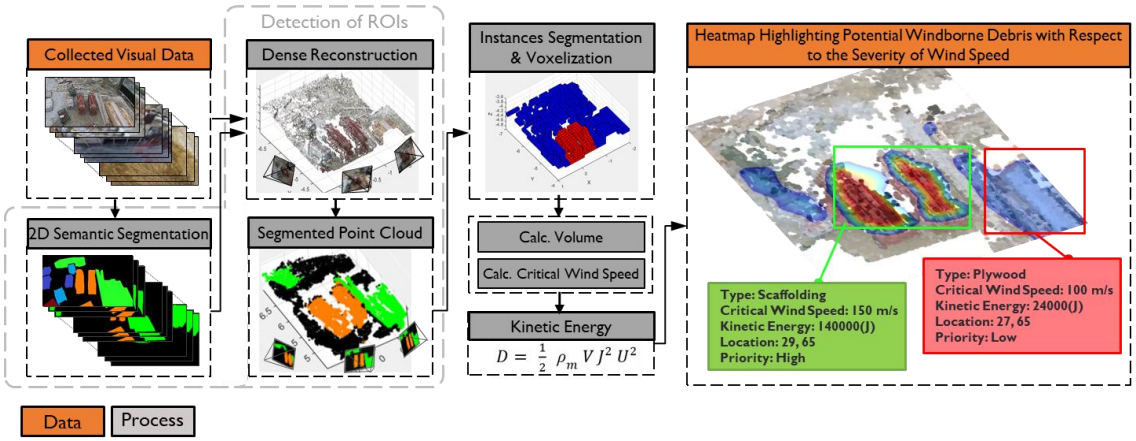

Figure 1. Overview of the proposed method to analyze potential risk of wind-induced damage in construction sites

3D Reconstruction of Construction Sites and Semantic Segmentation of ROIs

Building upon dense point cloud reconstruction of (Furukawa and Ponce 2009), we first reconstruct a 3D dense point cloud model of construction sites from images captured from UAVs. We then carry out the semantic segmentation over the collected images to identify ROIs at the 2D image level, and then project the outcome of the 2D semantic segmentation onto the point cloud model in order to detect ROIs in 3D. Projection of 2D imagery to 3D point cloud is achieved through identifying the association between the points of 3D point cloud models and the 2D image pixels. To establish such association using intrinsic and extrinsic camera parameters, we form the Equation (1) to represent the transformation.

$$C_i = K_{3\times3}[R_{3\times3} \mid T_{3\times1}]C_w \quad (1)$$

where R and T are the extrinsic parameters describing the rotation and translation of the camera, and K represents the intrinsic factors of the camera. The parameter C_w is the locations of the points in the 3D Cartesian system and C_i is the location coordinates of such points after projection with respect to the image center. Building upon equation (1), we read semantic values for each point from 2D segmented images. As the semantic class for a point is not always consistent among images, the most frequent class retrieved from the 2D images is considered as the semantic class of the point. Figure 2 illustrates the projection of semantic information from 2D to 3D.

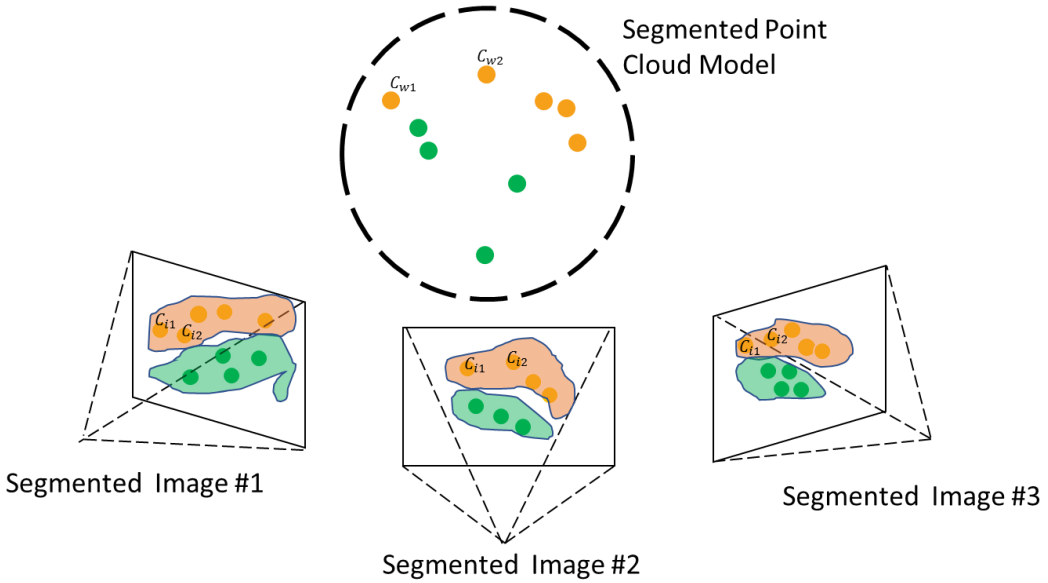

Figure 2. Projection of sematic information on the point cloud model.

A group of semantically segmented points in point cloud models will form an ROI. Thus, to process each ROI, it is essential to cluster all the points that represent the ROI. In this regard, we project the segmented point cloud model from the aerial perspective to a 2D grid of pixels in order to form an image. This process enables to generate bounding boxes to detect an ROI on a 2D image. We then map such bounding boxes onto the point cloud model to represent group of points belong to a particular ROI.

Volumetric Measurement of ROIs

In order to estimate the volume associated with an ROI, we transform the point cloud into a voxel space. Voxels are the lattice of regular grids that represent the occupancy of the points in 3D. A stack of voxels is used to pre-process the 3D geometries and represent their volumes (Maturana and Scherer 2015). To calculate the volume of an ROI, we detect the physical ground which the ROI is located upon, and then, the summation of the voxel volumes that are enclosed between the ROI and the ground represents the volume of an ROI. Mathematically, such workflow can be descried through the Equation (2):

$$Volume = v\sum_{i=1}^{n}\sum_{j=1}^{m}\mathrm{RetZ}((X_i, Y_j) \in R) - \mathrm{RetZ}((X_i, Y_j) \in \mathrm{G}) \quad (2)$$

where v is the volume of a single voxel, R and G are the coordinates of the voxel centers representing the ROI and the ground respectively, X_i, Y_j represent the coordinates of a voxel in XOY plan, and RetZ is the function that retrieves the Z value associated with a voxel which has coordinates of (X_i, Y_j, Z). The number of voxels in OX and OY directions are shown with n and m.

Calculation of Kinetic Energy of Wind-borne Debris Associated with ROIs

Once types of ROIs are identified and their volumes are calculated, the associated kinetic energy are analyzed. It is assumed that an ROI gains the corresponding kinetic energy once it is

lifted off the ground. Here, a critical wind speed that can lift off vulnerable objects associated with a specific ROI needs to be analyzed. According to (Wills et al. 2002), the critical wind speed for rod and plain type objects are defined in Equations (3) and (4) respectively:

$$Uc^2 = 2\left(\frac{\rho_m}{\rho_a}\right)\left(\frac{I}{C_F}\right)\lg \tag{3}$$

$$Uc^2 = \frac{\pi}{2}\left(\frac{\rho_m}{\rho_a}\right)\left(\frac{I}{C_F}\right)dg \tag{4}$$

where Uc is the critical wind speed, ρ_m and ρ_a are the density of the ROI and the air (kg/m^3), l is the thickness of plain type ROI (m), and d is the diameter of rod type objects (m), and g is the gravitational acceleration (m/s2), I indicates the bound coefficient associated with the ROI, and C_F is the drag coefficient.

Based on the estimated critical wind speed given any wind speed for each particular ROI, it is possible to analyze whether or not materials associated with a specific ROI become wind-borne debris. When wind speeds become greater than critical wind speed, vulnerable object associated with the ROI will be lifted off the ground, and related kinetic energy can be estimated through the Equation (5):

$$D = \frac{1}{2}\rho_m V J^2 U^2 \tag{5}$$

where D is the kinetic energy of the ROI (joules), V is the volume of the ROI (m^3) obtained through the volumetric measurement. The parameter U indicates the wind speed (m/s), and J is the ratio indicating the speed of wind-borne debris to the speed of wind.

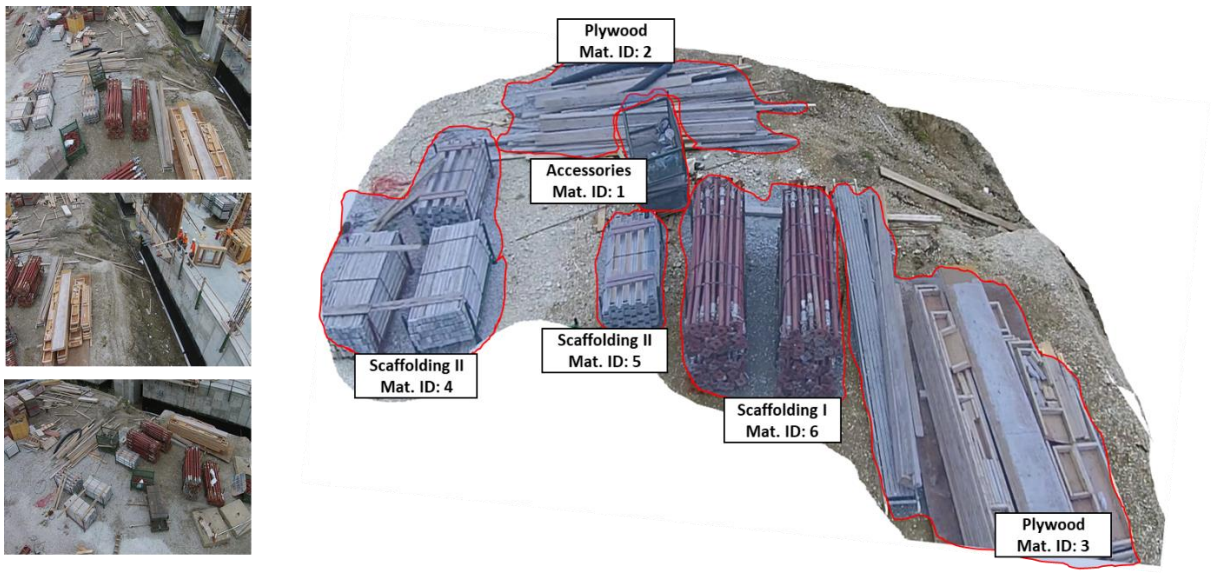

Figure 3. Examples of visual dataset collected from UAVs (left) and the types and IDs of materials in construction sites (right)

To better provide practitioners with insights on wind-induced damage with respect to the severity of the wind speed in construction sites, the outcome will be projected onto the point cloud model in the form of the heatmap-based visualization.

EVALUATION

In this study we have collected images from a construction site that contains wind-vulnerable materials consisting of two types of scaffoldings, metal accessories and plywood. We assume particular IDs to refer to each potential wind-borne debris as shown in Figure 3. In order to perform image-based 3D reconstruction, a total of 110 images were used (examples are shown in Figure 4.a). The semantic segmentation is performed on the 2D level imagery to identify the ROIs on those images. The outcomes are projected onto the point cloud model (Figure 4.b). The voxel representation is obtained from segmented point cloud data (Figure 4.c) and instance bounding box segmentation of ROIs are performed to extract each ROI in the voxel space. Objects formed by small number of voxel stacks are ignored to eliminate potential outliers.

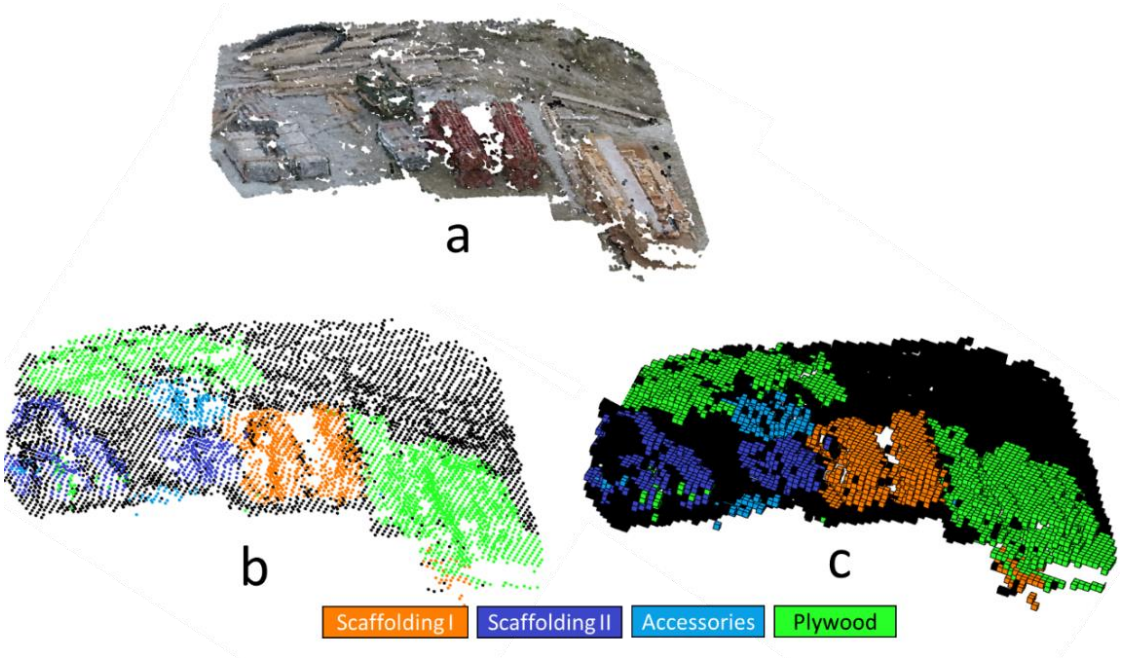

Figure 4. a) original point cloud, b) segmented point cloud, and c) corresponding voxel space

Table 1. Outcomes of the Proposed Volumetric Measurement in our Case Studies

IDs and Category types	This research (m^3) (Gird Size is 0.25 m)	Ground Truth(m^3)	Error (%)
ID: 1, Accessories	0.1302	0.1550	16.0%
ID: 2, Plywood	0.2004	0.2659	24.6%
ID: 3, Plywood	0.6214	0.7352	15.4%
ID: 4, Scaffolding II	0.2918	0.3559	18.0%
ID: 5, Scaffolding II	0.1253	0.1536	18.5%
ID: 6, Scaffolding I	0.4823	0.5658	14.7%

Volumetric measurement of vulnerable objects in ROIs is performed. The outcomes from the proposed method were compared with the ground truth (Table 1). The experimental results

indicate that the proposed method for volumetric measurement have satisfactory range of accuracy.

Building upon characteristics of objects in each ROI, the critical wind speed is estimated through the Equations (3) and (4). Table 2 represents the critical wind speed and parameters for each object.

Table 2. Parameters for Quantifying the Potential Threat in Terms of Kinetic Energy Associated with Potential Wind-borne Debris

Category Type	$\rho_m \left(\mathrm{Kg}/m^2\right)$	$d\left(m\right)$	$l\left(m\right)$	$Uc\left(m/s\right)$
Scaffolding I	2400	0.1	--	56.0
Scaffolding II	2000	0.1	--	51.1
Accessories	1000	0.5	--	20.0
Plywood	600	--	0.04	25.5

Finally, building upon Equation (5) and critical wind speeds for each ROI, a heatmap is generated to visualize their kinetic energy to analyze potential wind-induced damage in construction sites under different severity of the wind speeds (Figure 5).

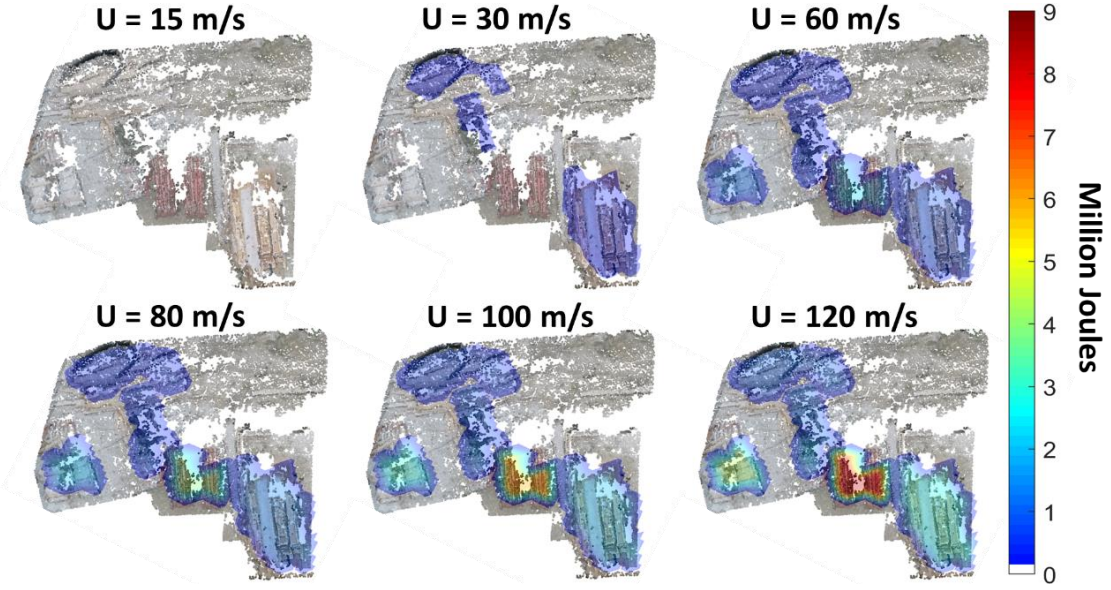

Figure 5. Kinetic energy associated with potential wind-borne debris to analyze wind-induced damage in different wind speeds

Figure 5 shows the threat and types of potential wind-borne debris in construction sites with respect to the severity of the wind event. In the case studies, the computation time was around 9 minutes, while the most computationally expensive process was the dense point cloud reconstruction. The outcome indicates that for a particular wind speed, there exists a unique heatmap illustrating the kinetic energy related to potential wind-borne debris. Thus, given a particular wind speed, this Imaging-to-Simulation model provides the rationale to determine the threat of wind-borne debris, and thus, enables practitioners to better secure their construction sites. Such systematic risk assessment will eliminate the subjective judgment of practitioners that mainly relies on their knowledge and empirical observations.

CONCLUSION

In this paper, we present a novel vision-based system to better secure construction sites by identifying and analyzing potential wind-induced damage in construction projects. Leveraging large-scale construction images from UAVs, we first construct a 3D point cloud of at-risk environments. Then, we detect potential wind-borne debris on the collected images and map them into the point cloud model. We convert the segmented point cloud model into the voxel space to perform the volumetric measurement of the potential wind-borne debris. Using the estimated volume, the type of materials and given wind speed, we estimate the critical wind speed and estimate the kinetic energy associated with vulnerable objects with respect to different wind speeds. Finally, a heatmap is generated to visualize dangerous areas/objects and inform practitioners for better preparedness prior to extreme wind events. This research enables practitioners to automatically flag vulnerable objects/areas with respect to the severity of extreme wind events, which helps better prepare at-risk environments in a timely manner. For future research, enhancements of the volumetric measurement part are needed to improve the reliability and scalability of this work. We are currently addressing the limitation of the voxelization process to increase the volumetric measurement accuracy. Also, we are interested in measuring the value of the proposed model and clarify how knowing the quantitative risk will reduce wind-induced damage in construction sites, in order to demonstrate the potential of this research. All of these are currently being carried out as our ongoing research.

ACKNOWLEDGMENT

This material is in part based upon work supported by the National Science Foundation (NSF) under CMMI Award #1832187. Any opinions, findings, and conclusions or recommendations expressed in this material are those of the authors and do not necessarily reflect the views of the NSF.

REFERENCES

Asadi, K., Ramshankar, H., Noghabaei, M., and Han, K. (2019). "Real-time Image Localization and Registration with BIM Using Perspective Alignment for Indoor Monitoring of Construction." *Journal of Computing in Civil Engineering*, 33(5), 04019031.

Asadi, K., Ramshankar, H., Pullagurla, H., Bhandare, A., Shanbhag, S., Mehta, P., Kundu, S., Han, K., Lobaton, E., and Wu, T. (2018). "Vision-based integrated mobile robotic system for real-time applications in construction." *Automation in Construction*, 96, 470-482.

Esmalian, A., Ramaswamy, M., Rasoulkhani, K., and Mostafavi, A. (2019). "Agent-Based Modeling Framework for Simulation of Societal Impacts of Infrastructure Service Disruptions during Disasters." *Computing in Civil Engineering 2019: Smart Cities, Sustainability, and Resilience*, American Society of Civil Engineers Reston, VA, 16-23.

Fermino, J. (2013). "Sandy caused $185M in damage to WTC site." <https://nypost.com/2013/03/20/sandy-caused-185m-in-damage-to-wtc-site>

Furukawa, Y., and Ponce, J. (2009). "Accurate, dense, and robust multiview stereopsis." *IEEE transactions on pattern analysis and machine intelligence*, 32(8), 1362-1376.

Ham, Y., and Kamari, M. (2019). "Automated content-based filtering for enhanced vision-based documentation in construction toward exploiting big visual data from drones." *Automation in Construction*, 105, 102831.

Ham, Y., Lee, S. J., and Chowdhury, A. G. (2017). "Imaging-to-simulation framework for

improving disaster preparedness of construction projects and neighboring communities." *Computing in Civil Engineering 2017*, 230-237.
Hatzikyriakou, A., Lin, N., Gong, J., Xian, S., Hu, X., and Kennedy, A. (2015). "Component-based vulnerability analysis for residential structures subjected to storm surge impact from Hurricane Sandy." *Natural Hazards Review*, 17(1), 05015005.
Holmes, J. (2004). "Trajectories of spheres in strong winds with application to wind-borne debris." *Journal of Wind Engineering and Industrial Aerodynamics*, 92(1), 9-22.
Holmes, J., Letchford, C. W., and Lin, N. (2006). "Investigations of plate-type windborne debris—Part II: Computed trajectories." *Journal of Wind Engineering and Industrial Aerodynamics*, 94(1), 21-39.
Kamari, M., and Ham, Y. "Automated Filtering Big Visual Data from Drones for Enhanced Visual Analytics in Construction." *Proc., ASCE Construction Research Congress 2018*.
Kareem, A. (1986). "Performance of cladding in Hurricane Alicia." *Journal of Structural Engineering*, 112(12), 2679-2693.
Lee, B. (1988). "Engineering design for extreme winds in Hong Kong." *Hong Kong Engineer*, 16(4), 15-23.
Maturana, D., and Scherer, S. (2015) "Voxnet: A 3d convolutional neural network for real-time object recognition." *Proc., 2015 IEEE/RSJ International Conference on Intelligent Robots and Systems (IROS)*, IEEE, 922-928.
Minor, J. E. (1994). "Windborne debris and the building envelope." *Journal of Wind Engineering and Industrial Aerodynamics*, 53(1-2), 207-227.
National-Oceanic-and-Atmospheric-Administration "Hurricane Costs." <https://coast.noaa.gov/states/fast-facts/hurricane-costs.html> (Jul. 26, 2019).
Smith, A. B., and Katz, R. W. (2013). "US billion-dollar weather and climate disasters: data sources, trends, accuracy and biases." *Natural hazards*, 67(2), 387-410.
Willison, C. E., Singer, P. M., Creary, M. S., and Greer, S. L. (2019). "Quantifying inequities in US federal response to hurricane disaster in Texas and Florida compared with Puerto Rico." *BMJ global health*, 4(1), e001191.
Wills, J., Lee, B., and Wyatt, T. (2002). "A model of wind-borne debris damage." *Journal of Wind Engineering and Industrial Aerodynamics*, 90(4-5), 555-565.